Enzyme-Based Photoelectrochemical Biofuel Cell

Linda de la Garza,[†] Goojin Jeong,[†] Paul A. Liddell,[†] Tadashi Sotomura,[‡] Thomas A. Moore,*[,†] Ana L. Moore,*[,†] and Devens Gust*[,†,§]

Department of Chemistry and Biochemistry, Arizona State University, Tempe, Arizona 85287-1604, and Advanced Technology Research Laboratories, Matsushita Electric Industrial Co. Ltd., Moriguchi, Osaka 570-8501, Japan

Received: March 21, 2003; In Final Form: June 24, 2003

Both dye-sensitized photoelectrochemical solar cells and biofuel cells are promising candidates for production of renewable energy. We have combined these two approaches into a single hybrid cell. The photoanode consists of a nanoparticulate SnO_2 electrode coated with a porphyrin sensitizer (**S**). Key to the operation of the cell is the coupling of the anode photoreactions to the oxidation of biological fuels such as glucose or alcohols by an NAD(P)H/NAD(P)$^+$ redox carrier. Electron donation to the oxidized sensitizer **S**$^{\bullet+}$ by NAD(P)H is facile, generating NAD(P)$^+$, which is not reduced by charge recombination reactions at the photoanode. Enzymes oxidize the biological fuel and, in the process, reduce the NAD(P)$^+$ coenzyme back to NAD(P)H. These reactions are coupled to cathodic redox reactions through an ion-permeable membrane in a two-compartment electrochemical cell. Hybrid cells of this general type have several potential advantages over either the photoelectrochemical cell or the biofuel cell operating individually.

Introduction

During photosynthesis, plants convert light energy into electrochemical energy and eventually into chemical potential energy stored in carbohydrates and other compounds. The carbohydrates are oxidized as needed to provide energy to the organism. Artificial analogues of these processes are being investigated as methods for electricity production.[1] For example, the initial steps in the photosynthetic process are mimicked by various photovoltaics, including dye-sensitized photoelectrochemical solar cells. The latter[2−4] employ nanoparticulate wide band gap semiconductor electrodes coated with monolayers of dye molecules that absorb light and inject electrons into the semiconductor. A different aspect of mimicry of biological energy transduction involves biofuel cells that produce electricity by oxidation of biological materials that can be produced by photosynthesis. These often use enzymes[5−9] or even entire organisms[7,10−12] to catalyze oxidation of carbohydrates and related materials, and couple the oxidation to electrical current flow between an anode and a cathode. Typical fuels that have been investigated include glucose[13−16] and methanol.[17,18]

Here, we introduce a new approach to mimicry of the photosynthetic process that involves a dye-sensitized nanoparticulate semiconductor photoanode working in combination with an enzyme-catalyzed biofuel cell. This system achieves simple and direct coupling of the two complementary processes, combines some of the advantages of each approach in a single unit, and can in principle provide more power than either process working independently.

Results

Photoelectrochemical Biofuel Cell. The cell is shown schematically in Figure 1. The basic concept begins with a nanoparticulate semiconductor electrode coated with a monolayer of an organic sensitizer dye (**S**) such as a porphyrin or chlorophyll. Excitation of the dye is followed by electron injection into the conduction band of the semiconductor and thus into the anode. This process produces an oxidized dye molecule. In our cell, this molecule is reduced back to its initial state by electron donation from the reduced form of nicotinamide adenine dinucleotide (NADH) or nicotinamide adenine dinucleotide phosphate (NADPH) that is present in the aqueous buffer solution bathing the electrode. Ultimately, two-electron oxidation of NAD(P)H by this process yields the stable oxidized form, NAD(P)$^+$. The NAD(P)$^+$ produced is not reduced at either the anode or the cathode but rather serves as an electron acceptor

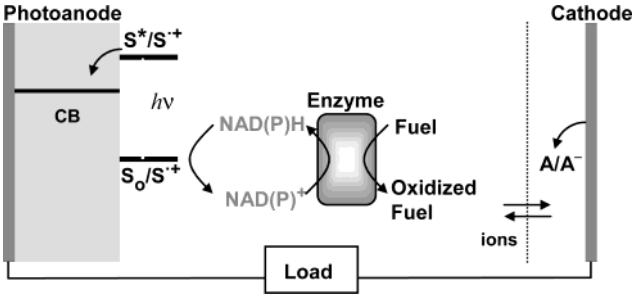

Figure 1. Schematic diagram of the hybrid cell. Upon irradiation of the photoanode, electrons are injected into the nanoparticulate SnO_2 coating the ITO conductive glass electrode from the excited state of porphyrin sensitizer **S**. The resulting **S**$^{\bullet+}$ is reduced by the reduced form of the redox couple (NAD(P)H). The resulting oxidized form of the couple (NAD(P)$^+$) is then reduced by a dehydrogenase enzyme, which uses a reduced carbon fuel as the source of electrons. This process produces more highly oxidized carbon-containing materials and hydrogen ions. The cathode used in these experiments was either a platinum gauze in the electrolyte or a separate Hg/Hg_2SO_4 electrode in saturated K_2SO_4 solution. In the two-compartment configuration, the half-cells are connected by a Nafion ion-permeable membrane sandwiched between two glass O-ring joints. The maximum cell voltage for a two-compartment cell of this general type depends on the choice of the cathodic half-cell.

* To whom correspondence should be addressed.
[†] Arizona State University.
[‡] Matsushita Electric Industrial Co. Ltd.
[§] E-mail: Gust@asu.edu.

10.1021/jp030360j CCC: $25.00
Published on Web 08/26/2003

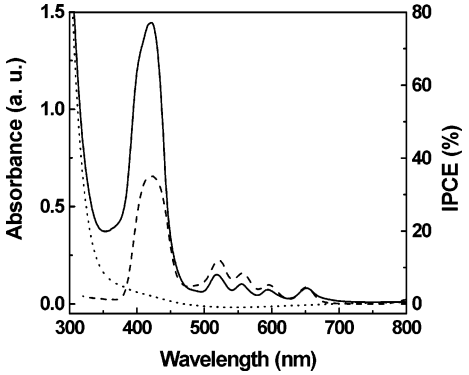

Figure 2. Absorption spectra of the bare photoanode consisting of nanoparticulate SnO_2 on ITO conductive glass (· · ·) and the same anode after coating with porphyrin sensitizer **S** (—). Also shown is the incident-photon-to-current-efficiency (IPCE) for a similar electrode in a photoelectrochemical cell as a function of wavelength (- - -), as discussed in the text.

for the enzymatic oxidation of a fuel such as glucose, methanol, or ethanol. This half-cell is coupled with either a simple platinum gauze cathode in the electrolyte solution or a separate cathodic half-cell via a Nafion perfluorosulfonate membrane. In operation, an electrical current flows between the photoanode and cathode, the organic fuel is oxidized (in some cases to CO_2), and charge is compensated by hydrogen ion flow through the membrane.

Photoanode. The photoanode consists of indium−tin oxide (ITO) coated conductive glass that bears a layer of nanoparticulate tin dioxide, $nSnO_2$. The $nSnO_2$ is coated with tetraarylporphyrin sensitizer **S** by soaking in a solution of the

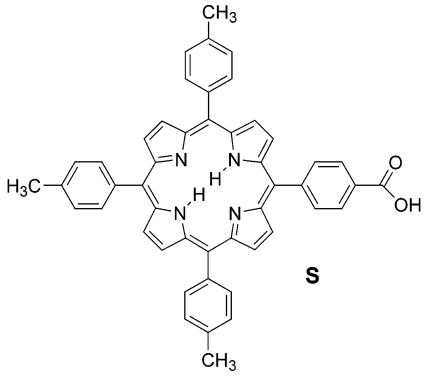

porphyrin in an organic solvent. The porphyrin presumably binds to the oxide through the carboxylic acid functionality. Porphyrins were chosen as our initial candidates for photosensitizers because they absorb light strongly in the visible, are chemically stable, can be easily modified in order to change their binding, absorption, or redox properties, have been extensively studied as components of molecular complexes designed to mimic photosynthetic electron transfer,[19] and have been investigated as components of dye-sensitized photoelectrochemical cells.[20−27] The absorption and light scattering curve of the bare nanoparticulate electrode, taken in air, is shown in Figure 2 as a dotted line. Note the absence of significant absorption in the visible region of the spectrum. After soaking the electrode in a solution of **S**, rinsing, and allowing the solvent to evaporate, the absorption spectrum shown by the solid line is observed. The spectrum features typical porphyrin absorption, with Q-bands at 650, 590, 555, and 520 nm, and a Soret band at ∼420 nm. The wavelength maxima are little changed from the absorption spectrum of **S** in toluene. However, the Q-bands are broadened slightly, and the Soret bands are broadened more significantly. This broadening may be due to interaction of the porphyrin with adjacent porphyrin molecules or with the semiconductor surface. The amplitude of the Soret band at 420 nm in Figure 2 may be somewhat distorted due to the high absorbance.

NAD(P)H/NAD(P)$^+$ Redox Couple. NADH and NADPH are in theory excellent redox mediators between the photoanode and the enzyme. They are involved as redox coenzymes in a large number of enzyme-mediated processes. They have been used as electron donors for reduction of a variety of oxidized organic compounds,[28−32] and they have highly reducing formal potentials that are suitable for reduction of the porphyrin radical cation resulting from electron donation into the photoanode by the sensitizer. Despite the potential advantages, NADH/NAD$^+$ has not proven to be a useful redox mediator for coupling enzymatic oxidations to the anode in biofuel cells. For fuel cell applications, NADH is not effectively oxidized at the usual electrodes such as platinum or glassy carbon due to a high overpotential and electrode fouling and irreproducibility.[6,28,33] For some applications, this problem can be reduced by the use of redox mediators to couple electrode reactions with NAD(P)H oxidation.[28,33] For example, it is possible to regenerate NAD$^+$ from NADH using the enzyme diaphorase, which is coupled to the anode by the redox mediator benzylviologen.[6] Alternatively, photochemical methods for NADH oxidation have been investigated, including the use of organic dyes[32,34,35] and band gap (UV) irradiation of TiO_2.[36]

We have found a novel solution to this problem. As illustrated below, we have observed that NADH is an excellent electron donor to the oxidized porphyrin sensitizer bound to the photoanode described above. Such a reaction has some precedent, as the zinc porphyrin radical cation formed by photoexcitation of a linked porphyrin−fullerene molecule has recently been reported to oxidize 1-benzyl-1,4-dihydronicotinamide, an NADH analogue, in organic solvents.[37] At pH = 7.0, the first oxidation potential of NADH is 0.73 V vs Ag/AgCl, [38] and NADH readily donates an electron to $\mathbf{S}^{\bullet+}$ (the first oxidation potential of **S** is 1.03 V vs Ag/AgCl). The second oxidation step of NADH is facile (−1.12 V), because the product of the initial one-electron oxidation, $NADH^{\bullet+}$, is highly acidic and, under neutral or basic conditions, rapidly deprotonates to yield $NAD^{\bullet}$. The radical is short-lived, and in the photoelectrochemical biofuel cell, it eventually undergoes a second electron transfer to an oxidized porphyrin to form NAD$^+$. This second oxidation step may involve the direct interaction of $NAD^{\bullet}$ with $\mathbf{S}^{\bullet+}$, disproportionation of partially oxidized species to yield NADH and NAD$^+$, or dimerization followed by oxidation of the dimer.[38,39] In the photoelectrochemical biofuel cell, NADPH behaves similarly.

The photoelectrochemical cell was set up as shown in Figure 1 with a platinum gauze cathode and an electrolyte consisting of aqueous 1.0 M NaCl containing 0.25 M Tris buffer at pH 8.0. The solution contained no enzymes or biofuel. The cell was illuminated with 520 nm light at 1.0 mW/cm^2, and the photocurrent was measured. In the absence of NADH, no significant photocurrent was observed. Adding increasing amounts of NADH to the solution led to increased photocurrents, until at 3.0 mM NADH or above, a limiting photocurrent of ∼35 μA/cm^2 was observed. The photocurrent was measured as a function of the wavelength of the exciting light, and the results were corrected for the power profile of the excitation system. The results are shown in Figure 2. The current production is plotted as the incident-photon-to-current efficiency (IPCE), which is defined as the number of electrons in the external circuit

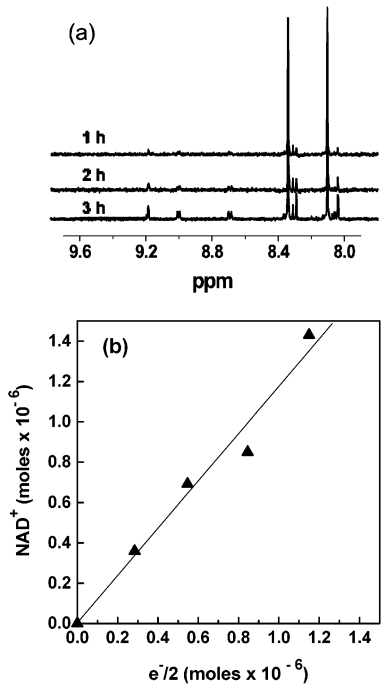

Figure 3. (a) ^{1}H NMR spectra showing the formation of NAD^+ from NADH in the photoelectrochemical cell with a platinum cathode. The times shown on the spectra signify hours of irradiation with 520 nm light prior to withdrawing the sample from the electrolyte solution. Spectra were taken in an 80/20 D_2O/H_2O mixture, using solvent suppression techniques to prevent interference from HOD. (b) Plot of the NAD^+ concentration, determined from calibration of ^{1}H NMR data similar to those shown in part a, vs half the number of electrons passing through the external circuit (▲). The solid line is a least-squares fit to the data.

generated by the cell divided by the number of incident photons. The IPCE tracks light absorption by the porphyrin in the Q-band region, indicating that light absorbed by **S** is responsible for the photocurrent. These experiments clearly demonstrate that NADH can act as an electron donor to the porphyrin radical cation produced by photoinduced electron transfer to the $nSnO_2$, leading to a significant photocurrent.

What are the products of NADH oxidation? To find out, the photoelectrochemical cell described in the last paragraph was prepared with H_2O containing 0.10 M sodium acetate as the electrolyte and an initial NADH concentration of 1.0 mM, and illumination at 520 nm was carried out for several hours with nitrogen purging. From time to time, aliquots of the electrolyte solution were withdrawn, and ^{1}H NMR spectroscopy was performed. Typical spectra in the downfield region are shown in Figure 3a. The upper spectrum was taken after 1 h of irradiation and shows two large resonances at 8.10 and 8.35 ppm that are characteristic of the adenine ring of NADH. With continued irradiation, new resonances grow in (lower spectra). Those in the 8.7−9.2 ppm region are due to the pyridine ring protons[40] of NAD^+. Continued irradiation results in increasing conversion of NADH to NAD^+, and no significant amount of other products is formed. A control experiment without illumination resulted in no significant conversion of NADH to NAD^+. The experiment was quantified by determining the amount of NAD^+ produced (determined from the calibrated NMR spectrum) as a function of the number of electrons flowing through the external circuit. A plot of the moles of NAD^+ produced versus half the number of electrons flowing is shown in Figure 3b. It is clear that NADH serves as a net two-electron donor and that the formation of NAD^+ is quantitative, within the accuracy of this measurement.

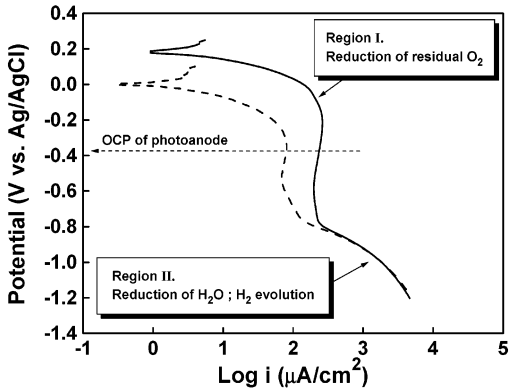

Figure 4. Cathodic potential vs current (logarithmic scale) for the platinum cathode in an aqueous solution containing 0.25 M Tris buffer (pH = 8.0), 0.10 M KCl, and 5.0 mM NADH. The potential was measured against a Ag/AgCl reference electrode, and the scan rate was 50 mV/s. The scans were performed in the presence of air (—) and after removal of some of the dissolved oxygen by purging with nitrogen (- - -).

These results show that NADH is a promising electron donor to the oxidized sensitizer, but they raise the question as to what reactions occur at the platinum cathode. We therefore measured the cathodic polarization behavior of the platinum cathode in the electrolyte described in the last paragraph. The results are shown in Figure 4. The highest-potential reduction feature is a function of the amount of oxygen dissolved in the sample and is ascribed to reduction of molecular oxygen. A second region, at lower potential, is independent of dissolved oxygen and is assigned to water reduction to yield hydrogen gas. We therefore conclude that the cathode reaction in the cells described above is reduction of dissolved oxygen.

Next, we examined the possibility of reduction of NAD^+ at the photoanode, which would limit cell performance. To determine the open circuit potential of the photoanode, a cell was prepared as described above and containing 5.0 mM NADH and 0.10 M KCl (in place of NaCl). Irradiation as described above yielded an open circuit potential of −0.37 V vs Ag/AgCl, as measured against a reference electrode inserted into the electrolyte solution. The one-electron reduction potential of NAD^+ is reported as −1.12 V vs Ag/AgCl.[39] This suggests that reduction of NAD^+ should not occur at the photoanode.

We also studied the cyclic voltammetry of a bare ITO electrode in 0.25 M Tris buffer at pH = 8.0 (Figure 5a). In the absence of NADH/NAD^+, no redox reactions were observed at potentials greater than ∼ −1.0 V vs Ag/AgCl, where hydrogen evolution was seen. When 10 mM NAD^+ was added to the cell, the reduction of NAD^+ was observed below −0.90 V. Similar experiments were carried out in the presence of NAD^+ with the ITO/$nSnO_2$ electrode (Figure 5b). The results were generally similar to those seen for ITO alone. There was a small amount of reduction at less negative potentials, and similar reduction was also observed with this electrode in the absence of NAD^+. It is ascribed to reduction of $nSnO_2$. With the ITO/$nSnO_2$ electrode, the reduction of NAD^+ occurs at a more negative potential than the open circuit potential of the photoanode, suggesting that reduction of NAD^+ at the photoanode via electrons injected into the conduction band by the photosensitizer is unlikely to be important for this cell configuration.

Taken together, these results show that although NADH functions well as an electron donor to $\mathbf{S}^{\bullet+}$ at the photoanode, NAD^+ is not efficiently reduced at either the photoanode or the platinum cathode. This is an ideal situation for the

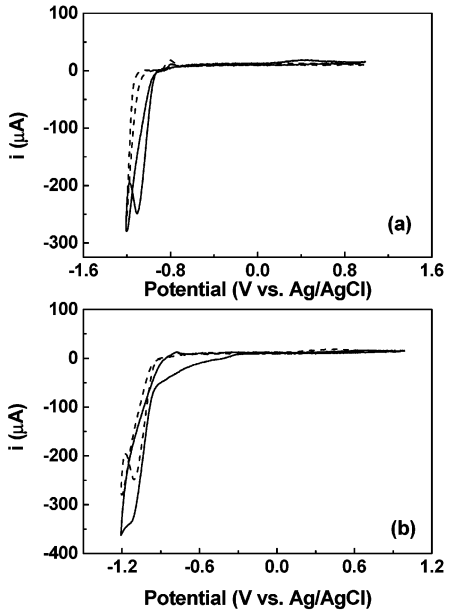

Figure 5. (a) Cyclic voltammetric results for an ITO conductive glass electrode measured in aqueous Tris buffer (0.25 M, pH = 8.0) (- - -) and for the same electrode in a similar solution which was also 10 mM in NAD^+ (—). The scan rate was 1.0 mV/s, and the counter electrode was Hg/Hg_2SO_4 in saturated potassium sulfate. (b) Cyclic voltammetric data taken under identical conditions as those in part a and with an electrolyte solution 10 mM in NAD^+. The electrodes measured were ITO conductive glass (- - -) and nanoparticulate SnO_2 sintered on ITO glass (—).

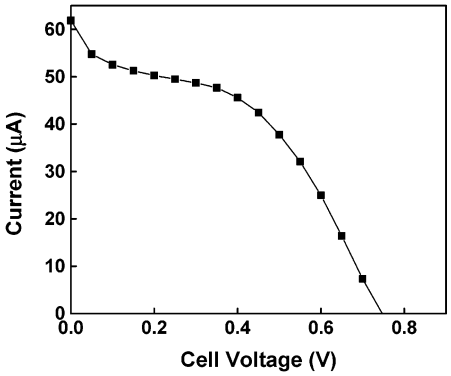

Figure 6. Current−voltage characteristics of the glucose-based photoelectrochemical biofuel cell prepared as shown in Figure 1 and employing the Hg/Hg_2SO_4 cathode in a two-compartment configuration. The electrolyte in the compartment containing the photoanode contained 0.25 M Tris buffer (pH = 8.0) and 0.10 M KCl, and the cell was irradiated with 1.0 mW/cm^2 light at 520 nm. The cell initially contained 4.0 mM NADH, 0.10 M β-D-glucose, and 0.015 units/mL GDH, and the measurement was taken after 1.0 h of irradiation with 1.0 mW/cm^2 of 520-nm light.

photoelectrochemical biofuel cell application, because performance-lowering recombination reactions are unlikely to occur with NAD^+. This result may be contrasted with the situation in dye-sensitized photoelectrochemical cells where I^-/I_3^- is used as the redox couple. In this case, the oxidized species, I_3^-, may be reduced at the photoanode, leading to energy-wasting recombination reactions and loss of efficiency.[41] Experiments with NADPH similar to those described above demonstrated that NADPH acts as an electron donor to $\mathbf{S}^{\bullet+}$ in a manner essentially identical to that of NADH.

Enzymatic Reactions. Although a variety of methods for regeneration of NAD(P)H from $NAD(P)^+$ have been investigated,[33,42−59] our application is designed to use the $NAD(P)^+$ produced at the photoanode in its biological role as an electron acceptor for enzyme catalyzed reactions. The result is oxidation of an organic fuel and production of the NAD(P)H needed to continue electron production at the photoanode. We have focused on the use of readily available, biologically derivable, reduced carbon compounds such as glucose, ethanol, and methanol. These can be oxidized enzymatically with various $NAD(P)^+$-requiring dehydrogenase enzymes. The final stage of oxidation of these compounds produces carbon dioxide. Below, we describe results with several of these systems.

Glucose as Fuel. Glucose dehydrogenase (GDH) oxidizes β-D-glucose to gluconolactone, consuming one molecule of NAD^+ and producing NADH and H^+ in the process. The gluconolactone hydrolyzes to gluconate in aqueous solution. Since GDH does not bind gluconate, the oxidation is not inhibited by the oxidation product. We have evaluated this initial step in the biological oxidation of glucose in the photoelectrochemical biofuel cell.

For these experiments, it was advantageous to use a nonpolarizable, highly reversible cathode so that restrictions of cathode redox reactions on the observed cell voltage and current would be minimized. The platinum cathode discussed above does not meet these requirements and limits cell performance under some conditions. We selected the well-known mercury/mercurous sulfate (Hg/Hg_2SO_4) electrode in saturated potassium sulfate solution, which possesses these characteristics. This electrode was interfaced with the photoanode compartment via a Nafion membrane, which is permeable to the hydrogen ions that must flow to maintain charge balance.

The photoanode compartment of this cell was prepared as shown in Figure 1. The electrolyte solution before irradiation contained 0.10 M KCl, 0.25 M Tris buffer at pH = 8.0, 4.0 mM NADH, 0.10 M β-D-glucose, and 0.015 units/mL GDH. The photoanode (2 cm^2 surface) was irradiated with 520 nm light at 1.0 mW/cm^2, and the cell current and voltage parameters were determined after 1 h of illumination (Figure 6). Under short circuit conditions, the cell produces $I_{sc} = 60\ \mu$A of current. At open circuit, the voltage V_{oc} is 0.75 V. A plot of power versus cell voltage shows that a maximum power P_{max} of 19 μW/2 cm^2 is obtained at 0.45 V. The fill factor, given by $P_{max}/I_{sc}V_{oc}$, is 0.42. The IPCE was 12% in this particular cell at 520 nm (the IPCE is wavelength dependent (see Figure 2)). Figure 6 demonstrates that the hybrid photoelectrochemical biofuel cell produces electricity when all of the components are in place, although no attempt to maximize cell performance has been made.

The useful effects of the enzyme and glucose are only expected to become apparent as the cell begins to convert significant amounts of NADH to NAD^+. To investigate this, we set up two cells as described above. One initially contained 4.0 mM NADH, and the second was identical but also contained 0.10 M β-D-glucose and 0.015 units/mL GDH. From time to time, samples were withdrawn from the cells to measure the NADH concentration. This was done by measuring its absorbance at 340 nm, where the extinction coefficient of NADH is 6.22 mM-cm^{-1}.[43] Figure 7a shows the NADH concentration in the electrolyte as a function of irradiation time. In the absence of glucose and GDH, the NADH concentration decreased with irradiation as it was oxidized to NAD^+ at the photoanode. When the same experiment was carried out with the addition of glucose and GDH, the concentration of NADH remained essentially constant over the entire 18-h period of illumination. Thus, the enzymatic system did indeed recycle the NADH via glucose oxidation. Figure 7b shows the moles of NADH consumed as a function of the moles of electrons produced in the external

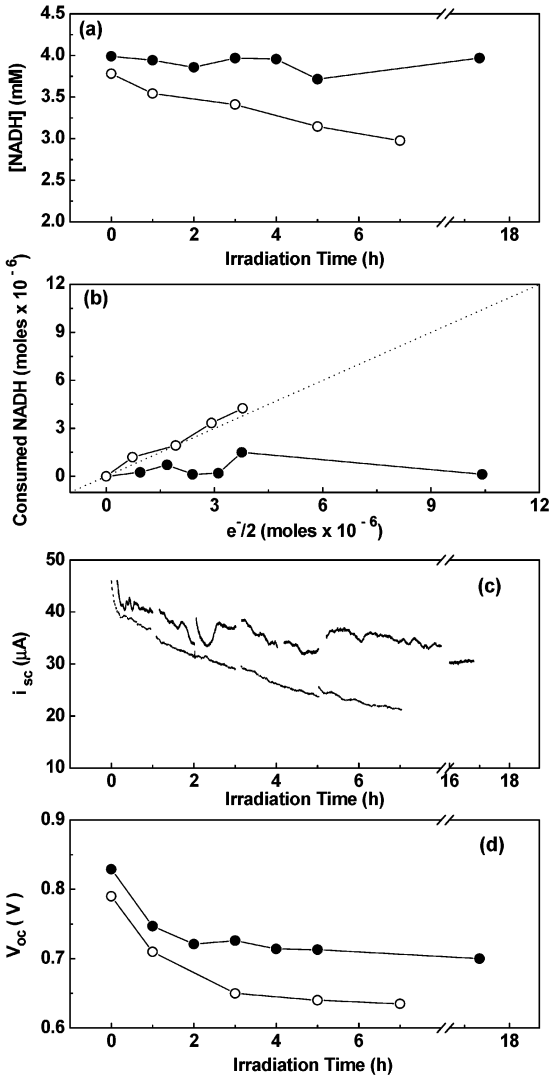

Figure 7. Performance of photoelectrochemical cell prepared as shown in Figure 1 and employing the Hg/Hg_2SO_4 cathode in a two-compartment configuration. The electrolyte in the compartment containing the photoanode contained 0.25 M Tris buffer (pH = 8.0) and 0.10 M KCl, and the cell was irradiated with 1.0 mW/cm^2 light at 520 nm. (a) The NADH concentration as a function of illumination time in a cell initially containing 4.0 mM NADH (○) or 4.0 mM NADH, 0.10 M β-D-glucose, and 0.015 units/mL GDH (●). (b) Moles of NADH consumed in the cell described above and initially containing 4.0 mM NADH (○) or 4.0 mM NADH, 0.10 M β-D-glucose, and 0.015 units/mL GDH (●), as a function of half of the number of electrons passing through the external circuit. (c) Photocurrent in the cell as described above and initially containing 4.0 mM NADH as a function of illumination time with (—) and without (· · ·) 0.10 M β-D-glucose and 0.015 units/mL GDH. The small gaps in the data are periods in which aliquots were withdrawn for measurement of the NADH concentration. (d) Open circuit photovoltage in the cell as described in part c with (●) and without (○) 0.10 M β-D-glucose and 0.015 units/mL GDH, as a function of irradiation time.

circuit. In the absence of enzyme and glucose, 1 mol of NADH was consumed for every 2 mol of electrons, as expected from the experiments discussed above.

Figure 7c and d addresses the change in cell performance with irradiation time. It is clear from Figure 7c that when glucose and GDH were present, the cell current was relatively constant with time, although some decrease in performance did occur over the 18-h irradiation period. On the other hand, the similar cell that did not contain the enzyme and glucose suffered a significant loss of current as the NADH was consumed. The

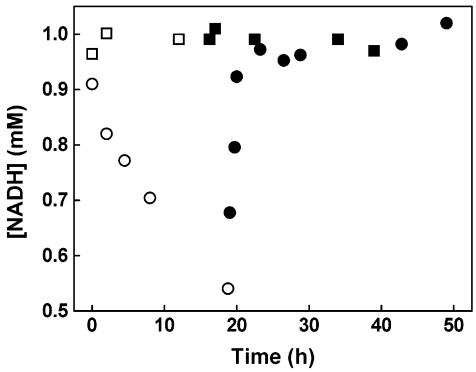

Figure 8. Concentration of NADH as a function of irradiation time for a cell prepared as in Figure 1 with a platinum cathode. The electrolyte solution contained 0.075 M Tris buffer (pH = 8.0) and 0.15 M NaCl, and the cell was irradiated with 0.50 mW/cm^2 light at 520 nm. Initially, the cell contained 1.0 mM NADH. With irradiation, the NADH concentration (○) decreased due to oxidation at the photoanode, while the NADH concentration in an identical cell that was not irradiated (□) was essentially unchanged. After 20 h, β-D-glucose (0.10 M) and GDH (0.015 units/mL) were added. The concentration of NADH was again monitored with (●) and without (■) irradiation.

effect on cell open circuit voltage is indicated in Figure 7d. In the presence of the enzyme and glucose, an initial decline in cell voltage over a period of 1 h was followed by a stable open circuit voltage of ~0.70 V that persists at 18 h. In the cell that lacked the enzyme and sugar, an initial rapid decline was followed by a continual reduction in cell voltage to 0.64 V after 8 h.

Additional evidence that the enzyme and glucose system is responsible for regeneration of the NADH consumed at the photoanode is shown in Figure 8. In this experiment, the cell, with the platinum cathode, contained 0.075 M Tris buffer at pH = 8.0, 0.15 M NaCl, and 1.0 mM NADH. It was illuminated for 20 h, whereupon nearly half of the NADH had been converted to NAD^+. At this time, 0.015 units/mL GDH and 0.10 M β-D-glucose were added. The NADH was rapidly regenerated by the enzymatic reaction, returning to its original concentration and remaining there during an additional 30 h of illumination. These data suggest that the cell can quickly recover from light-induced depletion of the electron donor when the enzyme and sugar are present.

Glucose-6-phosphate as Fuel. Glucose-6-phosphate dehydrogenase (G6PDH) catalyzes the oxidation of β-D-glucose-6-phosphate to 6-phosphoglucono-δ-lactone (which hydrolyzes to 6-phosphogluconate), with the corresponding reduction of $NADP^+$ to NADPH and production of H^+. A second enzyme, 6-phosphogluconate dehydrogenase (6PGDH), further oxidizes the 6-phosphogluconate to ribulose-5-phosphate, with the liberation of carbon dioxide and production of another equivalent of NADPH and H^+. Assays of these enzymes individually and in combination in the electrolyte solution of the photoelectrochemical biofuel cell demonstrated that they are both able to carry out their function under these conditions. These experiments and those in the complete cell described below were carried out at 35 °C, where turnover for 6PGDH is significantly more rapid than that at ambient temperatures.

The results of experiments with this enzyme system are shown in Figure 9. The photoelectrochemical cell was set up as described above, but with the platinum electrode. Initially, the concentration of NADPH was 1.0 M, and the cell contained no enzymes or substrate. Illumination of the cell resulted in consumption of the NADPH (accompanied by formation of $NADP^+$). After about half of the NADPH had been consumed,

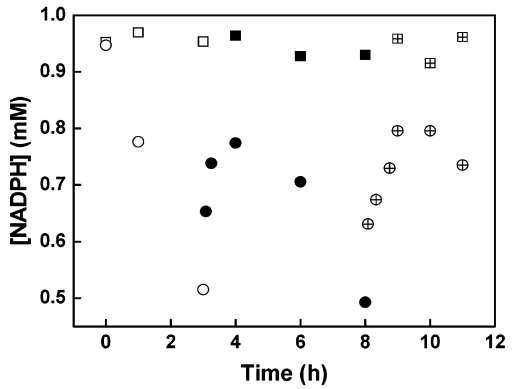

Figure 9. Concentration of NADPH as a function of irradiation time for a cell prepared as in Figure 1 with a platinum cathode. The electrolyte solution contained 0.25 M Tris buffer (pH = 8.0) and 0.10 M KCl, and the cell at 35 °C was irradiated with 1.0 mW/cm^2 light at 520 nm. Initially, the cell contained 1.0 mM NADPH. With irradiation, the NADPH concentration (○) decreased due to oxidation at the photoanode, while the NADPH concentration in an identical cell that was not irradiated (□) was essentially unchanged. After 3 h, β-D-glucose-6-phosphate (0.6 mM) and G6PDH (0.033 units/mL) were added. The concentration of NADPH was again monitored with (●) and without (■) irradation. At 8 h, 6PGDH (0.066 units/mL) was added, and the concentration of NADPH with (⊕) and without (⊞) illumination was monitored.

0.60 mM β-D-glucose-6-phosphate and 0.033 units/mL G6PDH were added. Even under continuing illumination, the enzymatic system regenerated a significant amount of NADPH via reduction of $NADP^+$. However, with increasing illumination time, the NADPH concentration began to decrease again due to consumption of the available β-D-glucose-6-phosphate and its conversion to 6-phosphogluconate. After a total of 8 h of illumination, the concentration of NADPH had again dropped to half of its initial value. At this time, 0.066 units/mL 6PGDH was added, and illumination was continued. The NADPH concentration increased as 6PGDH converted the 6-phosphogluconate to ribulose-5-phosphate, CO_2, and H^+, using $NADP^+$ as the electron acceptor. Thus, the two sequential enzymatic oxidation reactions regenerate NADPH in the functioning photoelectrochemical cell.

Methanol and Ethanol as Fuels. The results with β-D-glucose-6-phosphate demonstrate oxidation of a biofuel to carbon dioxide, and the two enzymatic reactions employed above are the only two reactions of the pentose phosphate pathway that generate reducing equivalents (NADPH). However, the carbohydrate oxidation product resulting from these reactions is still a 5-carbon sugar. A number of enzymatic reactions from the pentose phosphate pathway would be necessary to completely oxidize glucose to CO_2 in a biomimetic fashion. Therefore, we have also examined the use of simpler fuels in the photoelectrochemical biofuel cell. Methanol can be oxidized to formaldehyde by alcohol dehydrogenase (ADH), using NAD^+ as the electron acceptor. A second enzyme, aldehyde dehydrogenase (AlDH), uses NAD^+ to oxidize formaldehyde to formate, and a third, formate dehydrogenase (FDH), converts formate to carbon dioxide. Each oxidation step converts one molecule of NAD^+ into NADH.

The cell was prepared as described above, using the two-compartment configuration and the Hg/Hg_2SO_4 electrode. The electrolyte solution contained 0.9 mM NADH. After illumination of the photoanode for 20 h, almost all of the NADH was consumed (Figure 10). Addition of 5 vol % methanol, ADH (16.0 units/mL), AlDH (1.0 units/mL), and FDH (0.3 units/mL), with continued illumination, resulted in the return of the NADH concentration to its value prior to illumination. This is ascribed to the three enzymes acting in series. Evidence for this comes from the observation that the rate of regeneration of NADH in this experiment is more rapid than that in similar experiments that used only ADH, or ADH and AlDH. AlDH and FDH speed up the reaction not only by producing NADH from their respective substrates (and thereby adding to the production by ADH) but also by preventing product inhibition of the preceding enzyme in the series. A non-photochemical enzymatic assay in which each enzyme was added sequentially to a solution containing a limiting amount of NAD^+ showed that, under the conditions of the experiment, all three enzymes produce NADH from NAD^+.

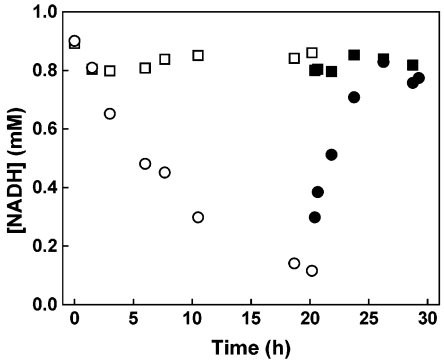

Figure 10. Concentration of NADH as a function of irradiation time for a cell prepared as in Figure 1 with the Hg/Hg_2SO_4 cathode. The electrolyte solution contained 0.25 M Tris buffer (pH = 8.0) and 0.10 M KCl, and the cell was irradiated with 0.50 mW/cm^2 light at 520 nm. Initially, the cell contained 0.90 mM NADH. With irradiation, the NADH concentration (○) decreased due to oxidation at the photoanode, while the NADH concentration in an identical cell that was not irradiated (□) was essentially unchanged. After 20 h of irradiation, 5 vol % methanol, ADH (16.0 units/mL), AlDH (1.0 units/mL), and FDH (0.30 units/mL) were added, and the NADH concentration was monitored with (●) and without (■) irradiation.

Experiments performed in a similar manner using ethanol as the fuel and the enzymes ADH and AlDH also demonstrated regeneration of NADH from NAD^+. The organic product was presumably acetate.

Discussion

These results demonstrate that it is possible to combine the function of a dye-sensitized nanoparticulate semiconductor electrode with that of a biofuel cell based on carbohydrate and dehydrogenase enzymes. The coupling factor is the NAD(P)H/$NAD(P)^+$ redox pair, which interfaces the one-electron reduction of the porphyrin radical cation produced by the photoinduced electron transfer reaction with the two-electron oxidations performed by the dehydrogenases. Previous attempts to use NADH as a redox mediator directly between an anode and dehydrogenase enzymes in biofuel cells have been thwarted by high overpotentials. Although no attempts have been made to optimize cell performance or the choice of cathode, the results obtained here are encouraging, with an open circuit voltage of 0.75 V and an incident-photon-to-current efficiency of 12% with 520-nm irradiation.

The unusual hybridization of a photoelectrochemical cell with a biofuel cell reaction requires both the oxidation of a reduced carbon fuel and light excitation. Such a combination has potential advantages over the individual approaches, each of which can generate electricity in its own right. In principle, a suitably designed hybrid cell could produce more power than either cell operating alone.

A hybrid cell can operate at a higher voltage, and therefore power, than a conventional fuel cell with the same fuel and the same cathodic half-cell (e.g., O_2 reduction). The anode potential in the hybrid cell is ultimately limited by the excited-state oxidation potential of the sensitizer dye (−0.67 V vs NHE for porphyrin **S**). Taking the formal potential of the oxygen-reducing half-cell as 0.82 V vs NHE at pH 7,[60] the thermodynamic maximum potential of the hybrid cell using sensitizer **S** is 1.49 V. However, the maximum realizable potential of the cell is actually limited by the conduction band/Fermi level of the semiconductor. Various semiconductors have been investigated as anode materials for photoelectrochemical cells.[3] The maximum potential for a hybrid cell using $nSnO_2$ and an oxygen cathode is 0.90 V at pH 7.0 (taking the conduction band edge as −0.07 V vs NHE[61]). If the $nSnO_2$ in the hybrid cell were replaceable by $nTiO_2$ (which is a commonly used nanoparticulate semiconductor in dye-sensitized photoelectrochemical cells), the maximum theoretical potential would be 1.40 V at pH 7.0 (taking the conduction band edge as −0.57 V vs NHE[3]).

Theoretically, direct oxidation of glucose in a biofuel cell would yield a maximum potential of 1.24 V, but such cells are currently unattainable. The maximum potential for indirect biofuel cells is dependent on the formal potential of the redox mediator in the anode compartment, as well as the potential of the cathodic half-cell. For example, an indirect cell using the $NADH/NAD^+$ couple and an oxygen cathode could theoretically produce a voltage of 1.14 V, based on formal potentials. As discussed above, this also is currently unrealizable. The benzylviologen-mediated cell mentioned above has a maximum theoretical potential of 1.1 V and actually realizes an open circuit voltage of 0.8 V.[6]

The hybrid cell can also theoretically operate at a higher voltage than a dye-sensitized photoelectrochemical cell using the same semiconductor and sensitizer. This is the case because the fuel cell configuration allows the use of a separate cathodic half-cell. The hybrid cell voltage is determined by the potentials of the cathodic half-reaction on one hand and the conduction band/Fermi level of the semiconductor on the other. In the dye-sensitized photoelectrochemical cell, the voltage is limited by the potentials of the redox couple carrying the current in the cell and the conduction band/Fermi level of the semiconductor. For example, typical dye-sensitized photoelectrochemical cells using $nTiO_2$ and the I^-/I_3^- redox couple have measured open circuit voltages of ∼0.8 V. As mentioned above, the two-compartment nature of the hybrid photoelectrochemical biofuel cell allows the use of a cathode that reduces highly oxidizing materials such as oxygen.

The hybrid cell has another potential advantage over the dye-sensitized photoelectrochemical cell. The I^-/I_3^- redox couple is usually employed in the best-known photoelectrochemical cells. The I_3^- resulting from reduction of the oxidized photosensitizer is reduced not only at the cathode (a necessity for current production) but also at the photoanode. This energy-wasting recombination reaction can limit the efficiency of the cell.[41] Designing a redox couple whose oxidized form was readily reducible at a cathode but inert toward reduction at the photoanode is a challenging task. In the cell described here, the oxidation product of NAD(P)H, $NAD(P)^+$, is not reduced at either the cathode or the photoanode, and hence, charge recombination at the photoanode by this mechanism does not occur. However, $NAD(P)^+$ is readily reduced back to NAD(P)H enzymatically, thus, in principle, permitting continuous current production until the reduced carbon fuel is expended.

Under certain conditions, the hybrid cell could in principle produce a higher current than a photoelectrochemical cell with the same semiconductor and sensitizer combination. At high light levels, efficiency in a traditional photoelectrochemical cell is limited not only by the wasteful reduction of the oxidized redox couple at the photoanode, as mentioned above, but also by mass transfer between the anode and cathode. After reduction of the oxidized sensitizer, an oxidized redox carrier must diffuse to the cathode before it can be reduced and recycled. In the hybrid cell, the reduction of $NAD(P)^+$ can be carried out in the immediate vicinity of the photoanode by the soluble enzyme system. Ideally, regeneration of NAD(P)H would only be limited by the diffusion of the reduced carbon fuel, whose concentration could be quite high. Of course, small, mobile ions such as hydrogen ions would still need to diffuse to the vicinity of the cathode to take part in the reduction of oxygen to water and maintain electrical neutrality.

Hybrid cells with suitable cathodes could be more environmentally friendly than many current cells, as they use water as the electrolyte and need not employ heavy metals and other toxic materials. The reduced carbon fuel could be obtained from many sources, including waste materials. The $NAD(P)^+$ produced by the photoanode could be harvested and used for supplying oxidizing power to a variety of enzymatic processes. Finally, the hybrid cell could, in principle, be used in conjunction with other electrodes and reactions to also generate electricity in the dark using more conventional fuel cell reactions.

Conclusion

These results show that it is possible to combine the chemistry of a dye-sensitized photoelectrochemical cell with that of an enzyme-catalyzed biofuel cell to prepare a hybrid cell that produces electric current when illuminated. The reactions at the photoanode are coupled to those of the fuel cell by NAD(P)H, which serves as a one-electron donor to oxidized photosensitizer molecules, ultimately producing $NAD(P)^+$, the two-electron oxidation product. The latter material serves as an electron-accepting coenzyme in the enzymatic oxidations and is thereby recycled to NAD(P)H. The anodic half-cell can be coupled to various cathodic half-cell reactions. The cell design overcomes problems due to high overpotentials for NADH oxidation at the anodes more commonly employed in biofuel cells and does not suffer from energy-wasting reduction of NAD^+ at the photoanode. Hybrid cells of this type offer several potential advantages over either the dye-sensitized photoelectrochemical cell or biofuel cells alone.

Experimental Section

Materials. Aqueous solutions were prepared with high purity water (Milli-Q-Nanopure). Solutions of $nSnO_2$ (15% aqueous SnO_2 colloidal particles, 15 nm average diameter) were obtained from Alfa Aesar. Toluene was distilled before use.

Enzymatic Assays. Before use, all enzymes were assayed for activity under the conditions of the experiment (buffer, salts, temperature, etc.) using standard assays. In each case, the formation of NAD(P)H was followed by absorption spectroscopy in a Shimadzu UV-1601 spectrometer with a temperature controlled cell holder. The concentration of NAD(P)H in the cell during operation was calculated using the absorption of the electrolyte solution at 340 nm and the extinction coefficient of NAD(P)H at that wavelength, 6.22 $mM \cdot cm^{-1}$.

Electrode Preparation. Nanoparticulate tin(IV) oxide electrodes ($nSnO_2$) were prepared by spraying a 1% aqueous solution of $nSnO_2$ (dilution of stock solution with 0.1% aqueous

ammonia) onto clean sheets of conductive glass, consisting of an indium-doped tin(IV) oxide (ITO) layer on a glass support (1×7 cm^2, sheet conductivity 10−12 Ω/cm^2, from Delta Technologies). After air-drying the electrode on a hot plate at ∼80 °C, the particles were sintered by heating in air at 400 °C for 1 h. The resulting electrodes were soaked in a solution of the sensitizer, 5-(4-carboxyphenyl)-10,15,20-(4-methylphenyl)-porphyrin (**S**),[62] in a 1:1 mixture of hexanes and toluene for 1 h, to form a molecular layer on the nanoparticulate surface. Electrodes were rinsed with clean solvents and dried under a stream of nitrogen.

UV−Vis Absorbance and NMR Spectroscopy. Absorption spectra of photoanodes were measured with a Shimadzu UV2100U UV−vis spectrometer. ^{1}H NMR spectra were obtained on a Varian Unity 500 MHz spectrometer. The solvent was a mixture of 80% D_2O and 20% H_2O, and solvent suppression techniques were used to eliminate interference from the HOD peak.

Photoelectrochemistry. Unless specified otherwise, the photoanode electrolyte was a nitrogen-purged aqueous solution of 0.10 M potassium chloride in Tris buffer (0.25 M, pH 8.0) that contained NAD(P)H as the redox relay. In the two-compartment cell, the Hg/Hg_2SO_4 electrode was bathed in a saturated potassium sulfate solution. Short circuit photocurrents were measured with a Keithley 617 electrometer as the difference in current observed with and without light incident on the backside of the $nSnO_2$/ITO photoanode. The counter electrode was a platinum gauze when a single cell compartment was used. With the two-compartment cell, a Hg/Hg_2SO_4 electrode was used as the cathode. Each compartment had a volume of 5 mL, and they were separated by a Nafion 117 ion exchange membrane clamped between two glass O-ring joints. Monochromatic light was provided by a Jobin-Yvon grating monochromator in line with a 450 W Osram xenon arc lamp powered by a 450 W power supply. The power density of the incident light as a function of wavelength was measured using a calibrated silicon diode detector (model 818-UV, Newport Research). Potentiostatic measurements were done with a PAR potentiostat. The reference electrode for three-electrode experiments was Ag/AgCl (0.2 V vs NHE). The current−voltage characteristics of the cells were measured using a Keithley 236 Source-Measure unit.

Acknowledgment. This work was supported by a grant from the Matsushita Electric Industrial Co., Ltd. This is publication 561 from the Arizona State University Center for the Study of Early Events in Photosynthesis.

References and Notes

(1) Dresselhaus, M. S.; Thomas, I. L. *Nature* **2001**, *414*, 332−337.
(2) O'Regan, B.; Grätzel, M. *Nature* **1991**, *353*, 737−740.
(3) Hagfeldt, A.; Grätzel, M. *Chem. Rev.* **1995**, *95*, 49−68.
(4) Sauve, G.; Cass, M. E.; Coia, G.; Doig, S. J.; Lauermann, I.; Pomykal, K. E.; Lewis, N. S. *J. Phys. Chem. B* **2000**, *104*, 6821−6836.
(5) Yahiro, A. T.; Lee, S. M.; Kimble, D. O. *Biochim. Biophys. Acta* **1964**, *88*, 375−383.
(6) Palmore, G. T. R.; Bertschy, H.; Bergens, S. H.; Whitesides, G. M. *J. Electroanal. Chem.* **1998**, *443*, 155−161.
(7) Palmore, G. T. R.; Whitesides, G. M. In *Enzymatic Conversion of Biomass for Fuels Production*; Himmel, M. E., Baker, J. O., Overend, P., Eds.; American Chemical Society Symposium Series 566; Washington, DC, 1994; pp 271−290.
(8) Katz, E.; Willner, I.; Kotlyar, A. B. J. *Electroanal. Chem.* **1999**, *479*, 64−68.
(9) Takeuchi, N. J. *J. Electrochem. Soc.* **1989**, *136*, 96−101.
(10) Karube, I.; Suzuki, S. *Methods Enzymol.* **1988**, *137*, 668−674.
(11) Tender, L. M.; Reimers, C. E.; Stecher, H. A., III; Holmes, D. E.; Bond, D. R.; Lowy, D. A.; Pilobello, K.; Fertig, S. J.; Lovley, D. R. *Nat. Biotechnol.* **2002**, *20*, 821−825.
(12) Park, D. H.; Zeikus, J. G. *Appl. Microbiol. Biotechnol.* **2002**, *59*, 58−61.
(13) Gongotri, K. M.; Regar, O. P.; Lal, C.; Kalla, P.; Genwa, K. R.; Meena, R. *Int. J. Energy Res.* **1996**, *20*, 581−585.
(14) Chen, T.; Calabrese Barton, S.; Binyamin, G.; Gao, Z.; Zhang, Y.; Kim, H. H.; Heller, A. *J. Am. Chem. Soc.* **2001**, *123*, 8630−8631.
(15) Katz, E.; Filanovsky, B.; Willner, I. *New J. Chem.* **1999**, 481−487.
(16) Mano, N.; Mao, F.; Heller, A. *J. Am. Chem. Soc.* **2002**, *124*, 12962−12963.
(17) Daubmann, T.; Aivasidis, A.; Wandrey, D. *Water Sci. Technol.* **1997**, *36*, 175−182.
(18) Yue, P. L.; Lowther, K. *Chem. Eng. J.* **1986**, *33*, B69−B77.
(19) Gust, D.; Moore, T. A. In *The Porphyrin Handbook*; Kadish, K. M., Smith, K. M., Guilard, R., Eds.; Academic Press: New York, 2000; pp 153−190.
(20) Kalyanasundaram, K.; Vlachopoulos, N.; Krishnan, V.; Monnier, A.; Grätzel, M. *J. Phys. Chem.* **1987**, *91*, 2342−2347.
(21) Dabestani, R.; Bard, A. J.; Campion, A.; Fox, M. A.; Mallouk, T. E.; Webber, S. E.; White, J. M. *J. Phys. Chem.* **1988**, *92*, 1872−1878.
(22) Kay, A.; Grätzel, M. *J. Phys. Chem.* **1993**, *97*, 6272−6277.
(23) Fungo, F.; Otero, L.; Durantini, E. N.; Silber, J. J.; Sereno, L. E. *J. Phys. Chem. B* **2000**, *104*, 7644−7651.
(24) Koehorst, R. B. M.; Boschloo, G. K.; Savenije, T. J.; Goossens, A.; Schaafsma, T. J. *J. Phys. Chem. B* **2000**, *104*, 2371−2377.
(25) Boschloo, G. K.; Goossens, A. *J. Phys. Chem.* **1996**, *100*, 19489−19494.
(26) Bedja, I.; Hotchandani, S.; Carpentier, R.; Fessenden, R. W.; Kamat, P. V. *J. Appl. Phys.* **1994**, *75*, 5444−5446.
(27) Bedja, I.; Kamat, P. V.; Hotchandani, S. *J. Appl. Phys.* **1996**, *80*, 4637−4643.
(28) Gorton, L. *Chem. Soc., Faraday Trans.* **1986**, *82*, 1245−1258.
(29) Taraban, M. B.; Kruppa, A. I.; Polyakov, N. E.; Leshina, T. V.; Lusis, V.; Muceniece, D.; Duburs, B. *J. Photochem. Photobiol., A: Chem.* **1993**, *73*, 151−157.
(30) Polyakov, N. E.; Taraban, M. B.; Kruppa, A. I.; Avdievich, N. I.; Mokrushin, V. V.; Schastnev, P. V.; Leshina, T. V.; Muceniece, D.; Duburs, G. *J. Photochem. Photobiol., A: Chem.* **1994**, *74*, 75−79.
(31) Martens, F.; Verhoeven, J. W.; Gase, R. A.; Pandit, U. K.; De Boer, T. *Tetrahedron* **1978**, *34*, 443−446.
(32) Martens, F. M.; Verhoeven, J. W. *Recl. Trav. Chim. Pays-Bas* **1981**, *100*, 228−236.
(33) Chenault, H. K.; Simon, E. S.; Whitesides, G. M. *Biotechnol. Genet. Eng. Rev.* **1988**, *6*, 221−271.
(34) Chambers, R. P.; Ford, J. R.; Allender, J. H.; Baricos, W. H.; Cohen, W. *Enzyme Eng.* **1974**, *2*, 195−202.
(35) Koper, N. W.; Jonker, S. A.; Verhoeven, J. W.; van Dijk, C. *Recl. Trav. Chim. Pays-Bas* **1985**, *104*, 296−302.
(36) Aoki, A.; Ueda, M.; Nakajima, H.; Tanaka, A. *Biocatalysis* **1989**, *2*, 89−95.
(37) Fukuzumi, S.; Imahori, H.; Okamoto, K.; Yamada, H.; Fujitsuka, M.; Ito, O.; Guldi, D. M. *J. Phys. Chem. A* **2002**, *106*, 1983−1908.
(38) Moiroux, J.; Elving, P. J. *J. Am. Chem. Soc.* **1980**, *102*, 6533−6538.
(39) Carlson, B. W.; Miller, L. L.; Neta, P.; Grodkowski, J. *J. Am. Chem. Soc.* **1984**, *106*, 7233−7239.
(40) Bakker, C. J.; de, G.; Verhoeven, J. W.; De Boer, Th. J. *Recl. Trav. Chim. Pays-Bas* **1975**, *3*, 61−74.
(41) Ferber, J.; Stangl, R.; Luther, J. *Sol. Energy Mater.* **1998**, *53*, 29−54.
(42) Aizawa, M.; Coughlin, R. W.; Charles, M. *Biochim. Biophys. Acta* **1975**, *385*, 362−370.
(43) Bresnahan, W. T.; Elving, P. J. *Biochim. Biophys. Acta* **1981**, *678*, 151−156.
(44) Long, Y. T.; Chen, H. Y. *J. Electroanal. Chem.* **1997**, *440*, 239−242.
(45) Aizawa, M.; Suzuki, S.; Kubo, M. *Biochim. Biophys. Acta* **1976**, *444*, 886−892.
(46) Baik, S. H.; Kang, C.; Jeon, I. C.; Yun, S. E. *Biotechnol. Tech.* **1999**, *13*, 1−5.
(47) Karyakin, A. A.; Bobrova, O. A.; Karyakina, E. E. *J. Electroanal. Chem.* **1995**, *399*, 179−184.
(48) Kim, S.; Yun, S. E.; Kang, C. *J. Electroanal. Chem.* **1999**, *465*, 153−159.
(49) Matsue, T.; Chang, H. C.; Uchida, I.; Osa, T. *Tetrahedron Lett.* **1988**, *29*, 1551−1554.
(50) Cantet, J.; Bergel, A.; Comtat, M. *Mol. Catal.* **1992**, *73*, 371−380.
(51) Gros, P.; Zaborosch, C.; Schlegel, H. G.; Bergel, A. *J. Electroanal. Chem.* **1996**, *405*, 189−195.
(52) Umeda, K.; Nakamura, A.; Toda, F. *J. Chem. Soc., Chem. Commun.* **1990**, 885−886.

(53) Bojarska, E.; Pawlicki, K.; Czochralska, B. *J. Photochem. Photobiol., A: Chem.* **1997**, *108*, 207−213.
(54) Dicosimo, R.; Wong, C. H.; Daniels, L.; Whitesides, G. M. *J. Org. Chem.* **1981**, *46*, 4622−4623.
(55) Wong, C. H.; Whitesides, G. M. *J. Am. Chem. Soc.* **1981**, *103*, 4890−4899.
(56) Wong, C. H.; Whitesides, G. M. *J. Org. Chem.* **1982**, *47*, 2816−2818.
(57) Wong, C. H.; Whitesides, G. M. *J. Am. Chem. Soc.* **1983**, *105*, 5012−5014.
(58) Pollak, A.; Blumenfeld, H.; Wax, M.; Baughn, R. L.; Whitesides, G. M. *J. Am. Chem. Soc.* **1980**, *102*, 6324−6336.
(59) Cuendet, P.; Grätzel, M. *Photochem. Photobiol.* **1984**, *39*, 609−612.
(60) Pourbaix, M. *Atlas of Electrochemical Equilibria in Aqueous Solutions*; National Association of Corrosion Engineers: Houston, TX, 1974.
(61) Nasr, C.; Kamat, P. V.; Hotchandani, S. *J. Phys. Chem. B* **1998**, *102*, 10047−10056.
(62) Anton, J. A.; Kwong, J.; Loach, P. A. *J. Heterocycl. Chem.* **1976**, *13*, 717−725.